Early Cretaceous intraplate seamounts from Guanajuato, central Mexico: geochemical and mineralogical data

Luis Enrique Ortiz-Hernández*, Otilio Arturo Acevedo-Sandoval, and Kinardo Flores-Castro

Centro de Investigaciones en Ciencias de la Tierra, Universidad Autónoma del Estado de Hidalgo, Carretera Pachuca-Tulancingo Km. 4.5, C.P. 42184, Pachuca, Hgo. México
** leoh@uaeh.reduaeh.mx*

ABSTRACT

An Early Cretaceous submarine volcanic and volcaniclastic sequence is found in the northwestern part of the Sierra de Guanajuato, in central Mexico. This sequence is formed by mildly alkaline basaltic pillow lavas interbedded with massive lava flows, pillow breccias, hyaloclastites, lapilli tuffs, and cognate feeder dikes capped by ribbon cherts and other pelagic flysch-like sediments.

Mineralogically, the pillow lavas and cognate diabasic dikes are composed of titaniferous salite/augite, albite, ilmenite, titanite, prehnite, and pumpellyite. Geochemically, they are characterized by high contents of TiO_2, Zr, Nb, and P_2O_5, high Ti/V ratios (49-61), and slightly enriched LREE-patterns ($2 < La_N/Yb_N < 4$). These rocks are interpreted as remnants of shallow water deposits of intra-plate seamounts formed as a result of hot-spot volcanism.

Keywords: Pillow lavas, seamounts, hot-spot, Early Cretaceous, Guanajuato, Mexico.

RESUMEN

Una secuencia marina volcánica y volcaniclástica del Cretácico Inferior ocurre en la porción noroccidental de la Sierra de Guanajuato, México central, y está formada de lavas basálticas almohadilladas ligeramente alcalinas intercaladas con lavas masivas, brechas almohadilladas, hialoclastitas, tobas de lapilli y diques diabásicos cogenéticos que están sobreyacidos por pedernales bandeados y otros sedimentos pelágicos flyschoides.

Las lavas almohadilladas y los diques diabásicos cogenéticos presentan salita/augita titanífera, albita, ilmenita, titanita, prehnita y pumpellita. Desde el punto de vista químico las rocas se caracterizan por contenidos altos de TiO_2, Zr, Nb, P_2O_5, cocientes Ti/V altos (49-61), y por patrones ligeramente enriquecidos en tierras raras ligeras ($2 < La_N/Yb_N < 4$). Estas rocas son interpretadas como remanentes de agua somera de montes submarinos intra-placa, formados como resultado de un vulcanismo de punto caliente.

Palabras clave: Lavas almohadilladas, montes submarinos, punto caliente, Cretácico Inferior, Guanajuato, México central.

INTRODUCTION

Studies of seamounts and other associated sedimentary deposits are important in order to understand the topography, sedimentological evolution and petrological characteristics of oceanic plates. In the 80s, such studies were revolutionized by submersible observation of seamounts (Londsdale and Batiza, 1980). Staudigel and Schmincke (1984) have proposed a tectonic model for seamount evolution, taking as example the Pliocene seamount La Palma series in the Canary Islands.

The Late Jurassic-Early Cretaceous Arperos Formation, exposed on the northwestern side of the Sierra de Guanajuato in central Mexico, is interpreted in this paper as a hot-spot seamount with flanking sediments. It provides an excellent opportunity for examining the geochemical and mineralogical data of an intra-plate seamount. This article focuses on field, mineralogical, and geochemical data from pillow lavas and diabasic dikes of the Arperos Formation seamounts, and discusses them with regard to the evolution of the Arperos oceanic intraplate basin (Freydier *et al*., 1996; Freydier *et al*., 1998; Freydier *et al*., 2000). We summarize the field relationships of these rocks, some aspects of their major and trace-element geochemistry, and the compositions of unalterated clinopyroxene phenocrysts. We then discuss the implications of these rocks for the tectonic setting of the paleovolcanic series of central Mexico.

GEOLOGICAL SETTING AND AGE OF THE SEQUENCE

The Sierra de Guanajuato, located in central Mexico, lies in the central segment of the Guerrero terrane. The northwestern part of the Sierra de Guanajuato includes the Comanja de Corona region (Figures 1 and 2), which was studied by Chiodi *et al*. (1988) and Quintero-Legorreta (1992). The geological framework of the Sierra consists of a collage of both Cordilleran and Tethyan sequences, Late Jurassic-Early Cretaceous in age. The Guanajuato magmatic sequence is formed by a cogenetic island arc tholeiitic suite, ranging from ultramafic-mafic cumulate rocks, through diabasic feeder dikes, to basaltic pillow lavas (Lapierre *et al*., 1992) thrust to the NNE, over a contemporaneous, highly deformed flysch-like detrital and volcanic sequence. This sequence is the Arperos Formation (Monod *et al*., 1990), composed of

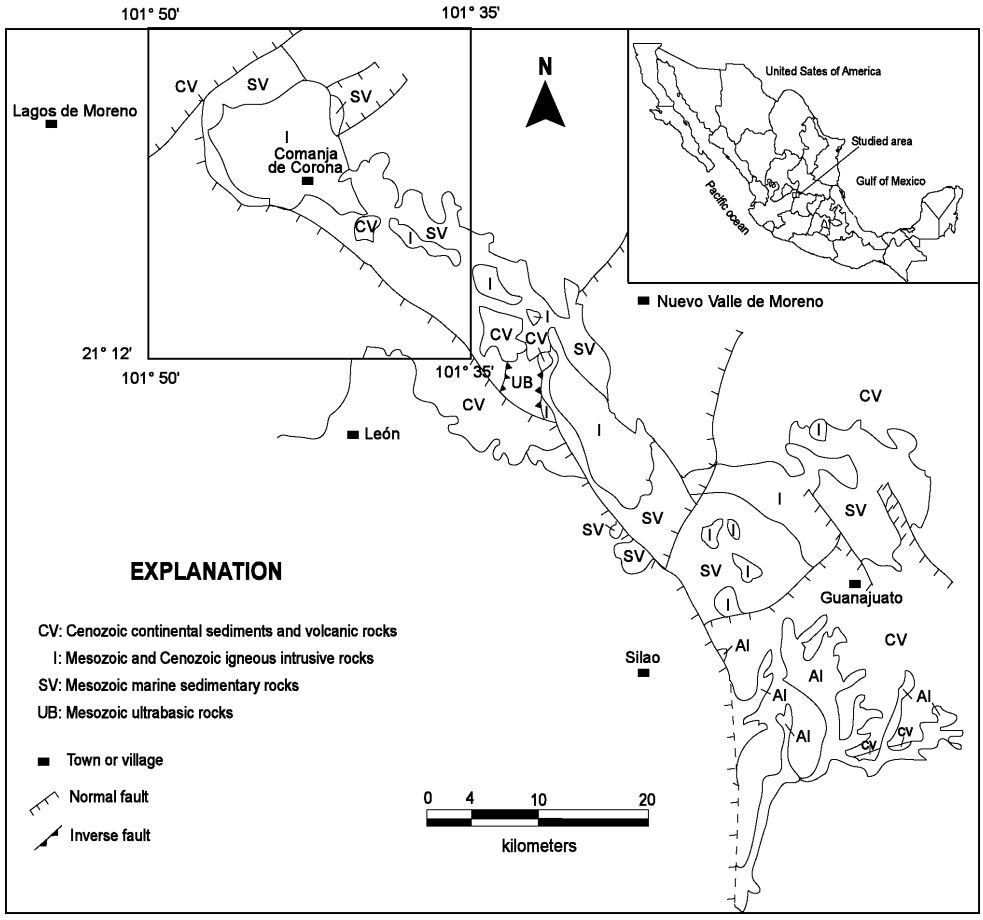

Figure 1. Geological sketch map of the Sierra de Guanajuato showing the location of the studied area.

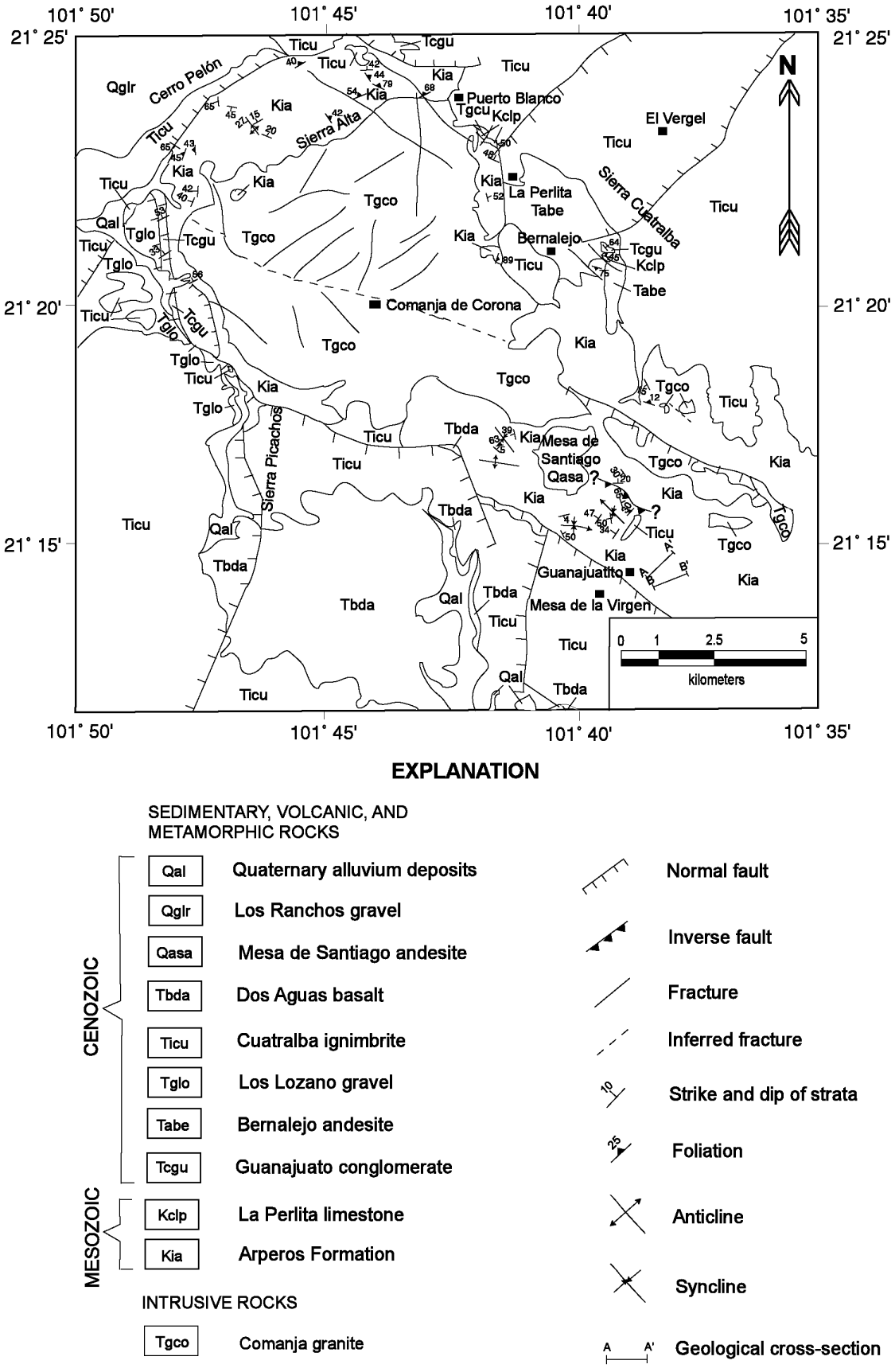

Figure 2. Geological map of the Comanja region (after Quintero-Legorreta, 1992).

graywackes, quartzites, micritic limestones, radiolarian cherts, black shales, and rare conglomerates, resting conformably over pillow lavas, diabasic dikes, and volcaniclastic rocks (Figure 3). The Arperos Formation shows isoclinal folds with E-W axial planes carried to the NNE. It forms the lowermost tectonic unit of the Sierra de Guanajuato, and the most extended, with outcrops exposed between the Jalisco-Guanajuato state boundary and the Guanajuato mining district, over a distance of 80 kilometers.

Radiolaria recovered from the cherts of the Arperos Formation, near the town of same name, have been tentatively assigned a Valanginian-Turonian age (Dávila-Alcocer and Martínez-Reyes, 1987). Nannofossils in the lowermost limestone levels suggest a Tithonian-Hauterivian age for the base of this formation (Corona-Chávez, 1988).

Chiodi *et al*. (1988) and Quintero-Legorreta (1992) reported Aptian-Albian neritic limestones 15 kilometers northeast of the city of León. This is La Perlita limestone (about 100 m thick), which carries Tethyan fauna and, in the Puerto Blanco outcrop (Figure 2), rests in angular unconformity on the Arperos Formation (Figure 3).

Fossils recovered at this site are reworked gastropoda and pelecypodes, including *Ceritium bustamantii* and *Psilothyris occidentalis* of Neocomian-Aptian-Albian age, and one brachiopod (*Peregrinella*) of lower Hauterivian age (Ortiz-Hernández and Martínez-Reyes, 1993). *Peregrinella* is a benthic index fossil, related to vent biota and black smokers, commonly associated with transform faults (Lemoine *et al*., 1982). It is a typical enigmatic Tethyan fossil that may have hopped seamounts across the circum-Pacific (Ager, 1993). The occurrence of *Peregrinella* in Mexico would support a transatlantic connection (Sandy, 1991). However, its record from Pacific-located suspect terranes (Sandy and Blodgett, 1996) does not necessarily confirm this. The occurrence of *Psilothyris occidentalis* supports an Aptian-Albian age for La Perlita limestone (Sandy, verbal communication, 1995).

On the northwestern side of the sierra (Comanja de Corona region), geological cross sections exposed in the Guanajuatito and Barbosa creeks (Figure 4) are considered as the type locality of the volcanic part of the Arperos Formation. The sequence is almost 400 m thick and is formed by basaltic pillow lavas interbedded with hyaloclastites and pillow breccias (Figure 5) intruded by diabasic dikes. These rocks are capped upward by pelagic sediments including ribbon cherts, shales, graywackes, and rare basaltic sills (Figure 6). These rocks were thrust over micritic limestones of undetermined age, considered to be an intermediate member of the

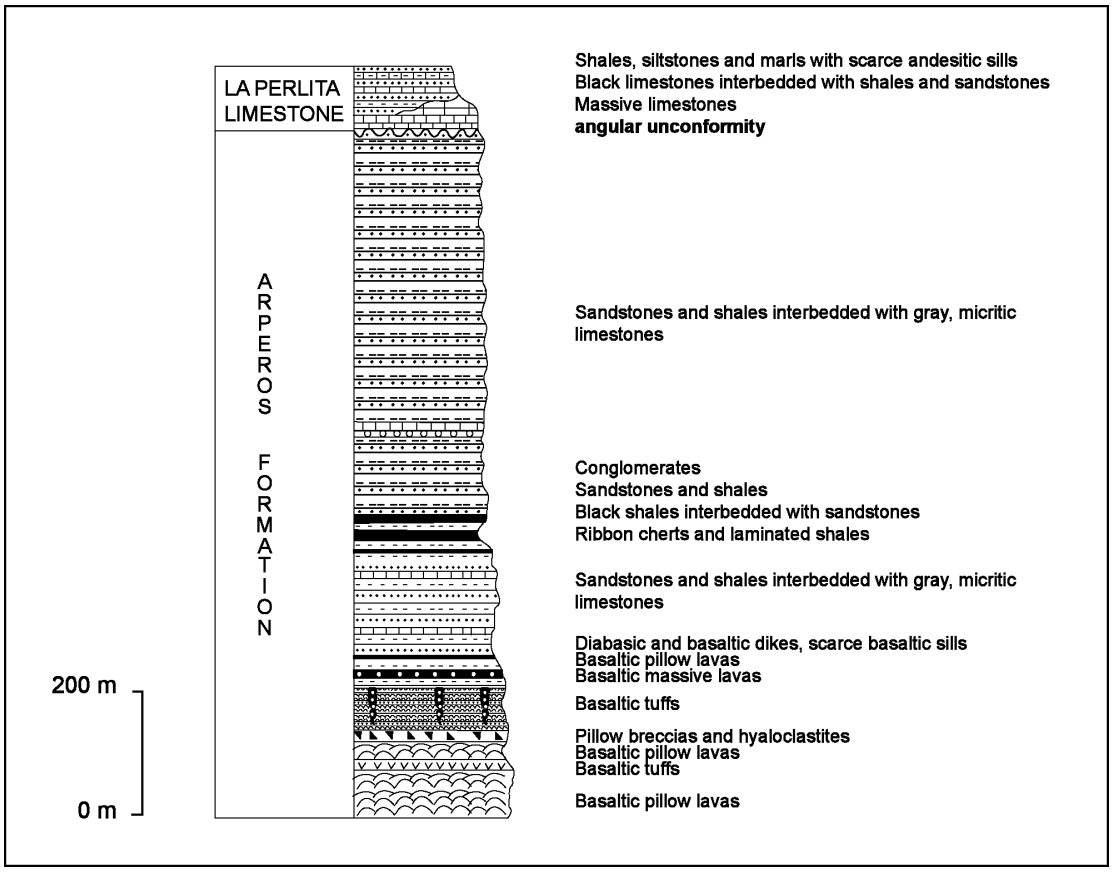

Figure 3. Simplified lithostratigraphy of the Lower Cretaceous Arperos Formation and La Perlita limestone.

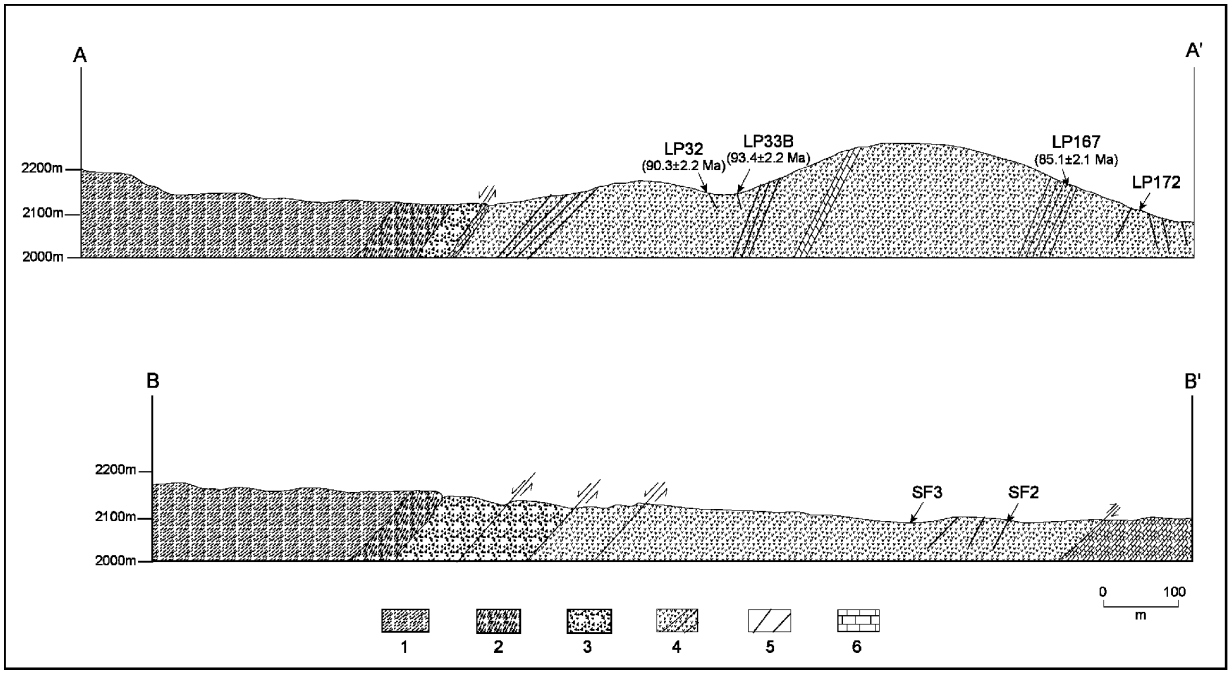

Figure 4. Geological cross sections in the Guanajuatito (A-A') and Barbosa (B-B') creeks showing the location of studied samples and their K/Ar radiometric ages. 1: Pelagic sediments; 2: Cherts and siltstones; 3: Mafic tuffs and hyaloclastites; 4: Basaltic pillow and massive lavas; 5: Diabasic and basaltic dikes; 6: Micritic limestones of undetermined age.

same formation (Quintero-Legorreta, 1992). They are affected by normal faults striking NNW and dipping to the NE. This assemblage of rocks was considered to be part of a Triassic ophiolitic sequence: the "Barbosa ophiolite" (Quintero-Legorreta, 1992). As later discussed, the results from this study are not in accordance with that interpretation.

Pillow lavas have devitrified glassy rims transformed to chlorite. The pillows are 30-50 cm wide, and display radial cracks and abundant vesicles filled by chlorite or calcite, by light-gray micritic limestones, or by rare chert as inter-pillow material. Scarce elongated pillow tubes also occur in the pillow horizons. Pillow lava horizons are separated by brownish-reddish oxidation zones, indicating emplacement in shallow water. The diabasic dikes are cross-cut by veins of prehnite-quartz or by pumpellyite-bearing assemblages. Thin basaltic sills (35 cm) were intruded into the pelagic sediments. The occurrence of micritic limestone in the pillow horizons suggests that these rocks were formed above the carbonate-compensation depth (CCD).

Pillow breccias consist of highly-vesiculated,

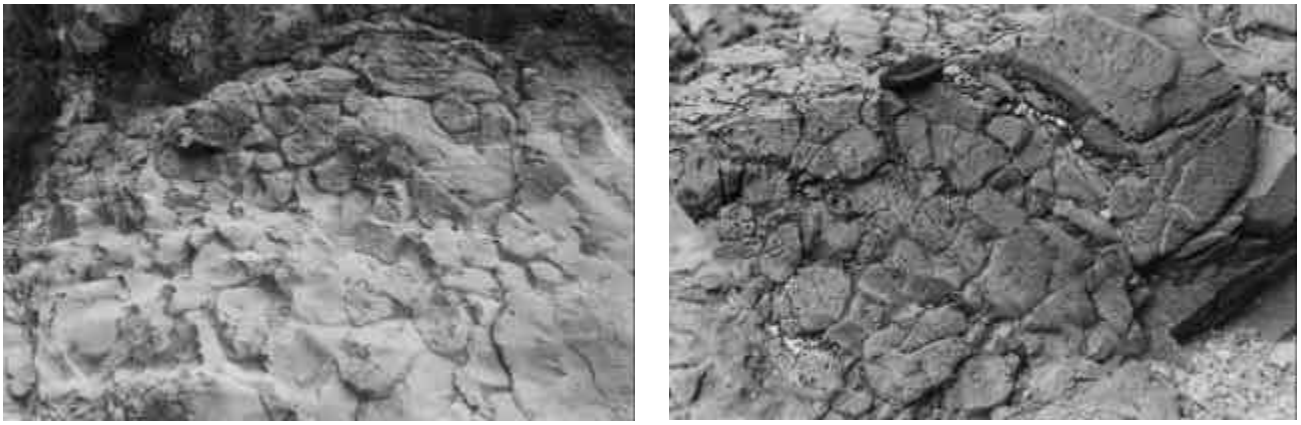

Figure 5. Pillow lavas and pillow breccias with glassy rims and vesicular structure in the Guanajuatito creek. Pillow diameters are approximately 30-50 cm. Hammer for scale.

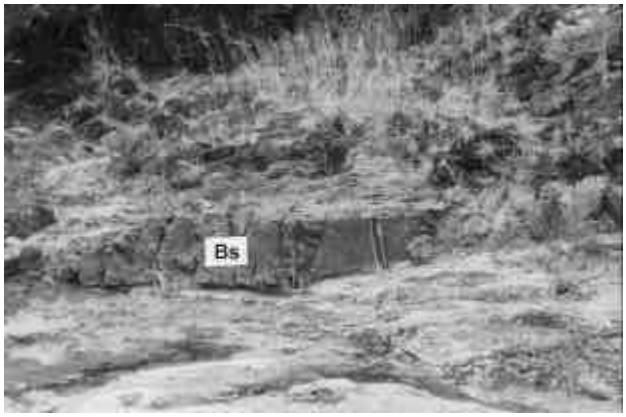

Figure 6. Basaltic sill (Bs) interbedded with ribbon cherts and laminated shales.

Figure 7. Hyaloclastites formed by subangular vitrous fragments interbedded with pillow tubes.

partly broken pillow lavas. The breccia matrix is fine-grained and formed by chlorite. Horizons (1-2 m wide) of massive basaltic lava also occur interbedded with the pillows. Hyaloclastites are formed by subangular to angular clasts of highly-vesiculated pumice lapilli and ash sized shards interbedded with pillow tubes (Figure 7). Ribbon cherts are present as a single 10 m thick horizon. Both massive and parallel-laminated beds of 1 to 10 cm thick chert are characteristic.

The conventional K-Ar dating method was applied to one basalt and two dikes from the Guanajuatito creek. K/Ar radiometric ages (whole-rock analyses) of the Arperos Formation record a wide range of ages (Table 1): 85.1±2.1 Ma for a pillow lava (sample LP-167) and 90.3±2.2 to 93.4 ±2.2 m.y. for two diabasic dikes (samples LP-32 and LP-33; Figure 4). These Turonian-Santonian ages are considered unreliable because the hydrothermal alteration and/or the low-grade metamorphism (prehnite-pumpellyite facies) affecting these rocks has probably produced uncertainty in the dating. This is corroborated by the high LOI of the analysed samples (3.51-5.25 wt %; see Table 2), indicating a high degree of alteration. A similar K/Ar radiometric age (82.6±5.4 Ma) was reported by Ortiz-Hernández *et al*. (1992) from an actinolitic hornblende in gabbro from the magmatic sequence of Guanajuato, which could constrain the age of metamorphism. On the other hand, significant excess of radiogenic ^{40}Ar has been reported in submarine basalts from two active Hawaiian volcanoes, Loihi Seamount and Kilauea (Honda *et al*., 1993). This significant excess of argon in volcanic rocks has been considered as inherited from the magmatic source. Olivine, clinopyroxene and plagioclase phenocrysts from basalts occluded argon within their mineral structures deep in the magma chamber and have retained this argon after emplacement and solidification of the lava (Laughlin *et al.,* 1994).

Stratigraphic relationships with the Aptian-Albian La Perlita limestone, and the fossil evidence in the sedimentary part of the volcanic and volcaniclastic sequence suggest a Late Jurassic-Early Cretaceous age for the Arperos Formation (Dávila-Alcocer and Martínez-Reyes, 1987; Corona-Chávez, 1988; Ortiz-Hernández and Martínez-Reyes, 1993).

Table 1. K/Ar isotopic data from basaltic pillow lava (sample LP-167) and diabasic dikes (samples LP-32 and LP-33). K determined by atomic absorption and Ar by isotope dilution using ^{38}Ar as spike. Decay constants: $\lambda\beta = 4.962 \times 10^{-10}$ years^{-1}; $\lambda\gamma = 0.581 \times 10^{-10}$ years^{-1}; $^{40}Ar = 0.01167$ % K.

Sample	K (%)	^{40}Ar rad. (10^{-6} cm^3/g)	$^{40}Ar/^{36}Ar$	Age ± 1 s (Ma)
LP-167	1.685	4.74	1461.5	85.1±2.1
LP-32	1.321	3.95	1675.0	90.3±2.2
LP-33	1.657	5.13	1757.7	93.4±2.2

PETROGRAPHY AND MINERALOGY

Analyses of clinopyroxene phenocrysts, plagioclase, and ilmenite were obtained on the automatized CAMEBAX microprobe electron at Grenoble University, France, with accelerating voltages of 15 kV and cup beam current of 10 ηA. All elements were counted for a maximum of 15 seconds. Under these conditions concentrations less than 0.2 wt% are considered as unreliable.

Brown clinopyroxene and plagioclase are the main phenocrysts in the lavas. Total phenocryst volume reaches 8% on the average. The matrix texture is interstitial with brown, pleochroic clinopyroxene, plagioclase microlites (Ab_{98}; Table 3), and orientated ilmenite crystals, usually transformed to titanite. Quench dendritic and skeletal crystals of clinopyroxene and plagioclase are common. A gray-blue pleochroic mineral pseudomorph of olivine crystals was identified as pumpellyite. Ilmenite contains 96% of ilmenite ($FeTiO_3$), and low geikielite ($MgTiO_3$) and hematite (Fe_2O_3) contents (Table 3). Diabasic dikes show the same mineralogy as the lavas and differ only in texture, being microlithic, porphyritic, or intergranular. They have subhedral phenocrysts of clinopyroxene and plagioclase surrounded by plagioclase microlites.

Clinopyroxene is the only magmatic mineral that is characteristically unaltered. It consists of titaniferous salites and rare titaniferous augites, with moderately high Al_2O_3 (2.4-7.2 wt. %) and TiO_2 contents (1.3-5.0 wt. %), relatively elevated Al/Ti ratios (1.9-4.2), and negligible Cr_2O_3 and NiO contents (Table 4). They are similar in composition to clinopyroxenes recorded in alkali basalts (Wass, 1979). The Di-Hd-En-Fs diagram shows that Mg enrichment ($58 \leq \#Mg \leq 77$) occurs at constant Ca contents and that Fe-enrichment is not present (Figure 8), which is a typical feature of alkaline series rocks (Barberi *et al*., 1971). Al^{IV}/Al^{VI} ratios suggest

Table 2. Chemical analyses of the pillow lavas (samples SF-3 and LP-167) and diabasic dikes (samples LP-172, LP-32, SF-2, and LP-33). Major elements in wt.% and trace elements in ppm.

	SF-3	LP-167	LP-172	LP-32	SF-2	LP-33
SiO_2	45.28	46.00	47.42	47.96	47.34	48.32
TiO_2	2.34	2.75	2.24	2.45	2.24	2.41
Al_2O_3	15.81	17.42	16.67	16.46	16.45	16.51
Fe_2O_3	10.09	10.46	10.30	9.21	9.75	9.66
MnO	0.12	0.11	0.15	0.14	0.13	0.15
MgO	7.00	6.33	6.90	6.22	6.99	6.45
CaO	5.36	4.72	6.61	8.30	6.33	6.49
Na_2O	4.02	4.23	4.24	4.16	3.52	4.19
K_2O	1.49	1.95	1.12	0.97	2.25	1.58
P_2O_5	0.47	0.55	0.44	0.34	0.48	0.40
LOI	8.01	5.25	3.74	3.51	4.27	3.59
TOTAL	99.99	99.77	99.83	99.72	99.75	99.75
Rb	17	20	13	11	17	16
Sr	333	201	323	304	576	281
Ba	146	106	97	138	121	143
Cr	113	250	157	212	146	137
Ni	91	147	101	43	94	44
V	238	278	220	302	206	258
Sc	29	29	30	43	30	36
Zr	153	266	192	215	180	206
Y	37	44	38	37	34	40
Nb	20	25	19	21	14	20
La	11.62	17.37	15.58	14.36	15.09	16.09
Ce	31.26	45.44	44.12	36.83	34.71	38.29
Nd	16.94	25.92	20.54	20.62	17.77	22.68
Sm	5.17	7.70	5.59	6.03	5.08	6.79
Eu	1.6	2.34	1.81	1.99	1.62	2.10
Gd	5.48	8.01	6.57	6.13	5.43	6.82
Dy	5.73	7.82	6.34	6.48	5.32	7.04
Er	3.00	3.79	3.37	3.21	2.91	3.40
Yb	2.88	3.97	3.02	3.38	2.63	3.62
Lu	0.58	0.69	0.58	0.56	0.33	0.59
$(La/Yb)_N$	2.72	2.95	3.48	2.87	3.87	3.00

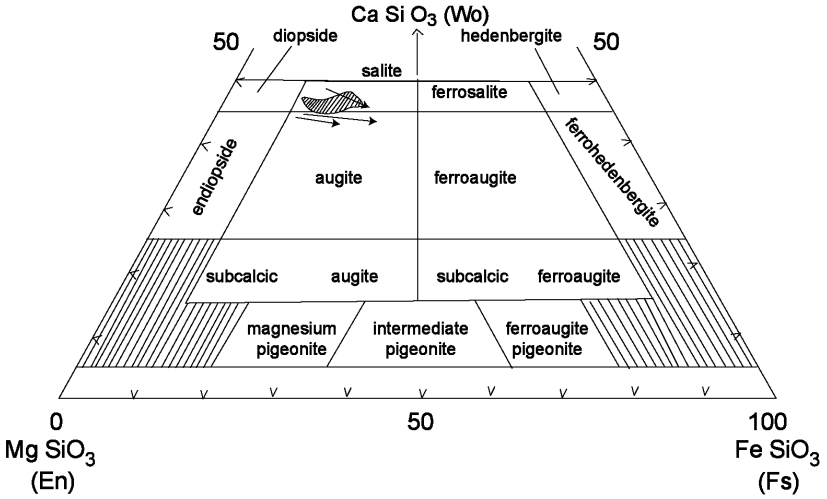

Figure 8. Classification of pyroxenes from Arperos diabasic dikes. Arrows show the evolution of alkalic series clinopyroxenes after Barberi *et al.* (1971).

Table 3. Chemical analyses of plagioclase and ilmenite for the Arperos diabases. Number of cations on the basis of 8 and 6 oxygens respectively. An=Anorthite, Ab=Albite, Or=Orthoclase, Il=Ilmenite, Gei=Geikielite, Hem=Hematite.

	SF-3	**SF-3**		**LP-36**	**LP-36**
SiO_2	69.15	68.01	TiO_2	49.72	49.72
Al_2O_3	19.24	19.84	Al_2O_3	0.05	0.26
FeO	0.01	0.01	Cr_2O_3	0.03	0.00
CaO	0.31	0.22	FeO	42.07	42.31
Na_2O	11.44	11.13	MnO	5.14	5.01
K_2O	0.05	0.08	MgO	0.10	0.07
TOTAL	100.20	99.29	TOTAL	96.61	97.37
Si	3.01	2.986	Ti	1.929	1.932
Al	0.987	1.027	Al	0.003	0.016
Fe	0.000	0.000	Cr	0.001	0.000
Ca	0.014	0.010	Fe^{3+}	0.138	0.121
Na	0.966	0.948	Fe^{2+}	1.694	1.707
K	0.003	0.004	Mn	0.227	0.219
TOTAL	4.980	4.976	Mg	0.008	0.005
			TOTAL	4.000	4.000
% An	1.47	1.08	%Il	95.70	96.30
% Ab	98.25	98.45	%Gei	0.50	0.30
% Or	0.28	0.47	%Hem	3.80	3.40

crystallization at intermediate to high pressures. The substitution of Al and Ti is the most important feature of these clinopyroxenes, as shown by their Si *vs.* Al and Al *vs.* Ti relations. Al and Ti enter into the pyroxene lattice in the form of Ti-Tschermakite component (TAL, $CaTiAl_2O_6$) via the coupled substitution $Ti^{4+}+2Al^{IV} \Leftrightarrow (Mg+Fe)^{2+}+2Si^{4+}$, which is the most important non-quadrilateral substitution in alkaline basalts (Almond, 1988). The NATAL ($NaTiSiAlO_6$) type substitution is less important in these clinopyroxenes as is shown in the Ti-Na-Al^{IV} ternary plot (Papike *et al*., 1974; Figure 9). High Al^{IV}/Al^{VI} ratios and high Na_2O contents is a characteristic of pyroxenes in alkalic basalts, where the Na (per formula unit) is combined with Ti as Na-^{VI}Ti (Tracy and Robinson, 1977). ^{VI}Ti-2^{IV}Al is the most important couple indicating an alkaline affinity of the host-rock. This couple is correlated with the low initial silica activity of the parental magma, with the crystallization of Ti-bearing oxide phases, but also with the degree of rock fractionation (Marcelot *et al*., 1988).

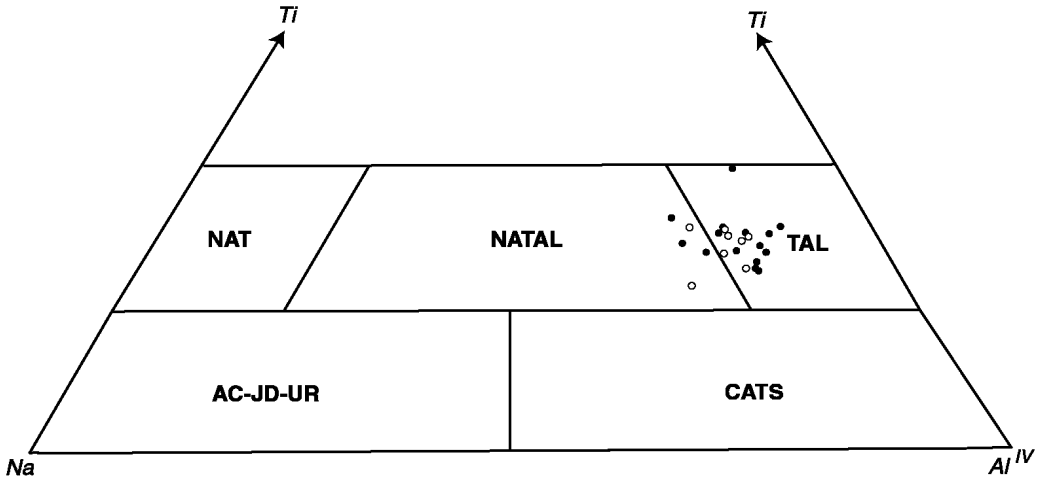

Figure 9. Composition of Arperos pyroxenes plotted on "others" diagram of Papike *et al.* (1974).

Table 4. Chemical analyses of clinopyroxene phenocrysts for the Arperos diabase, determined by microprobe (samples SF-5 and LP-36). Structural formulae calculated by stoichiometry to 6 oxygens and 4 cations, and Fe partition (not shown in the Table) calculated using the method of Papike *et al.* (1974).

	SF-5	**SF-5**	**SF-5**	**SF-5**	**SF-5**	**SF-5**	**SF-5**	**SF-5**	**SF-5**	**SF-5**	**SF-5**	**SF-5**	**SF-5**	**SF-5**	**SF-5**	**SF-5**	**LP-36**	**LP-36**	**LP-36**	**LP-36**	**LP-36**	**LP-36**
	c	c	c	c	c	c	r	c	c	c	r	c	r	c	r	c	c	r	c	r	c	r
SiO_2	49.71	50.34	49.6	50.51	51.8	48.91	50.65	48.59	49.53	49.18	50.06	48.43	47.91	47.45	49.33	49.67	43.81	50.2	46.03	48.27	47.74	48.02
TiO_2	2.24	1.84	2.34	1.84	1.96	2.56	2.20	4.37	2.43	2.46	2.31	3.14	3.04	3.41	2.72	2.42	5.04	1.34	3.65	1.86	2.04	2.22
Al_2O_3	3.85	4.96	5.56	4.98	3.91	5.65	4.53	5.21	5.25	4.96	4.84	6.45	6.24	6.07	5.69	3.69	7.19	2.44	5.36	3.26	4.00	3.52
Cr_2O_3	0.02	0.60	0.35	0.42	0.00	0.06	0.00	0.10	0.09	0.03	0.00	0.13	0.00	0.08	0.08	0.03	0.12	0.11	0.01	0.00	0.05	0.00
FeO	11.42	7.19	8.21	7.30	9.00	9.14	9.5	9.26	9.07	9.66	9.95	9.52	10.58	9.90	8.88	9.03	9.77	12.83	11.44	13.61	10.40	12.93
MnO	0.28	0.12	0.14	0.15	0.27	0.21	0.22	0.18	0.25	0.28	0.25	0.14	0.21	0.23	0.17	0.23	0.02	0.37	0.31	0.37	0.26	0.34
NiO	0.02	0.00	0.00	0.00	0.00	0.00	0.01	0.00	0.08	0.01	0.00	0.00	0.10	0.01	0.02	0.00	0.00	0.00	0.00	0.00	0.00	0.00
MgO	11.11	13.51	13.05	13.30	13.20	12.30	12.16	10.64	12.34	11.63	11.53	11.08	11.04	11.38	12.26	12.11	10.89	12.1	11.03	10.70	11.67	10.55
CaO	21.49	21.53	20.95	21.61	20.44	21.07	20.54	21.21	21.36	20.78	20.61	20.06	20.51	20.88	21.22	21.24	22.35	20.99	22.07	21.47	22.12	21.42
Na_2O	0.68	0.45	0.45	0.44	0.38	0.51	0.57	0.60	0.58	0.58	0.61	0.68	0.62	0.66	0.61	0.66	0.69	0.55	0.59	0.50	0.51	0.61
TOTAL	100.82	100.54	100.65	100.55	100.96	100.41	100.38	100.16	100.98	99.57	100.16	99.63	100.25	100.07	100.98	99.08	99.88	100.93	100.49	100.04	98.79	99.61
Si	1.866	1.857	1.834	1.862	1.905	1.823	1.882	1.820	1.837	1.852	1.871	1.817	1.802	1.787	1.826	1.877	1.673	1.895	1.753	1.854	1.834	1.847
Ti	0.063	0.051	0.065	0.051	0.054	0.072	0.061	0.123	0.068	0.070	0.065	0.089	0.086	0.097	0.076	0.069	0.145	0.038	0.105	0.054	0.059	0.064
Al	0.171	0.216	0.242	0.216	0.169	0.248	0.198	0.230	0.229	0.220	0.213	0.285	0.277	0.269	0.248	0.164	0.324	0.109	0.241	0.148	0.181	0.160
Cr	0.001	0.017	0.010	0.012	0.000	0.002	0.000	0.003	0.003	0.001	0.000	0.004	0.000	0.002	0.002	0.001	0.004	0.003	0.000	0.000	0.002	0.000
Fe	0.359	0.222	0.254	0.225	0.277	0.285	0.295	0.290	0.281	0.304	0.311	0.299	0.333	0.312	0.275	0.285	0.312	0.405	0.364	0.437	0.334	0.416
Mn	0.009	0.004	0.004	0.005	0.008	0.007	0.007	0.006	0.008	0.009	0.008	0.004	0.007	0.007	0.005	0.007	0.001	0.012	0.010	0.012	0.008	0.011
Ni	0.001	0.000	0.000	0.000	0.000	0.000	0.000	0.000	0.002	0.000	0.000	0.000	0.003	0.000	0.001	0.000	0.000	0.000	0.000	0.000	0.000	0.000
Mg	0.622	0.743	0.719	0.731	0.724	0.683	0.674	0.594	0.682	0.653	0.642	0.620	0.619	0.639	0.676	0.682	0.620	0.681	0.626	0.613	0.668	0.605
Ca	0.865	0.851	0.830	0.854	0.805	0.842	0.818	0.851	0.849	0.838	0.825	0.807	0.826	0.843	0.842	0.860	0.915	0.849	0.901	0.883	0.910	0.883
Na	0.050	0.032	0.032	0.031	0.027	0.037	0.041	0.044	0.042	0.042	0.044	0.049	0.045	0.048	0.044	0.048	0.051	0.040	0.044	0.037	0.038	0.045
TOTAL	4.007	3.993	3.990	3.987	3.969	3.999	3.976	3.961	4.001	3.989	3.979	3.974	3.998	4.004	3.995	3.993	4.045	4.032	4.044	4.038	4.034	4.031
%En	33.5	40.8	39.8	40.3	39.9	37.6	37.6	34.1	37.5	36.2	36.0	35.8	34.7	35.5	37.6	37.2	33.6	35.0	32.9	31.5	34.8	31.6
%Fs	19.8	12.4	14.3	12.7	15.7	16.1	16.8	17.0	15.9	17.4	17.9	17.5	19.0	17.7	15.6	16.0	16.9	21.4	19.7	23.1	17.8	22.3
%Wo	46.7	46.8	45.9	47.0	44.4	46.3	45.6	48.9	46.6	46.4	46.1	46.7	46.3	46.8	46.8	46.8	49.5	43.6	47.4	45.4	47.4	46.1
Al^{IV}	0.13	0.14	0.17	0.14	0.09	0.18	0.12	0.18	0.16	0.15	0.13	0.18	0.2	0.21	0.17	0.12	0.32	0.11	0.24	0.15	0.17	0.15
Al^{VI}	0.04	0.07	0.07	0.08	0.07	0.07	0.08	0.05	0.07	0.07	0.08	0.10	0.08	0.06	0.07	0.04	0.00	0.00	0.00	0.00	0.02	0.00
#Mg	63	77	74	76	72	71	70	67	71	68	67	67	65	67	71	71	67	63	63	58	67	59

Paleovolcanic series discriminant diagrams, using the Ti, Ca, Na, and Cr contents of the clinopyroxene phenocrysts (Leterrier, *et al*., 1982), show that the diabasic clinopyroxenes belong to an alkaline magma series, and that they were formed in an anorogenic setting (Figure 10).

GEOCHEMISTRY OF VOLCANIC ROCKS AND DIKES

Major elements were analyzed by X-ray fluorescence spectrometry. Trace elements including rare earth elements were analyzed by ICP-Atomic Emission Spectrometry at the Centre de Recherches Pétrographiques et Géochimiques in Nancy, France, following the analytical procedures of Govindaraju and Mevell (1987). Accuracy is estimated at 1% for major elements and 2% for trace elements. Loss on ignition (LOI) was performed at 900° C in a muffle furnace.

The rocks analyzed show typical features of alkali or mildly alkaline basalts, *i.e*., relatively high TiO_2 (> 2 wt%), P_2O_5 (> 0.30 wt%) and alkali content (Na_2O+K_2O > 5 wt%) (Table 2). In the scheme of the TAS classification, the lavas are basanites and hawaiites whereas the dikes are classified as hawaiites and alkaline basalts. Nevertheless, it is highly probable that the concentration of alkalis does not correspond to primary concentrations in the rocks due to hydrothermal alteration or metamorphism. The abundance of large cations such as Ba, Sr and Rb is low, but similar to typical alkali basaltic rocks (200 < Ba < 1400 ppm; 400 < Sr < 4000 ppm, and 15 < Rb < 100 ppm) (Basaltic Volcanism Study Project, 1981). Transition metals (Cr, Ni, Sc) also have low values. Ni values range from 43-147 ppm whereas Cr values vary between 113-250 ppm (Table 2). Cr/Ni ratios vary from 1.24 to 4.95 and V/Sc ratios from 6.87 to 9.59. Zr and Nb values are close to those of ocean island alkali basalts (200 < Zr < 1000 ppm, 20 < Nb < 160 ppm, and 5 < Zr/Nb < 15) (Basaltic Volcanism Study Project, 1981).

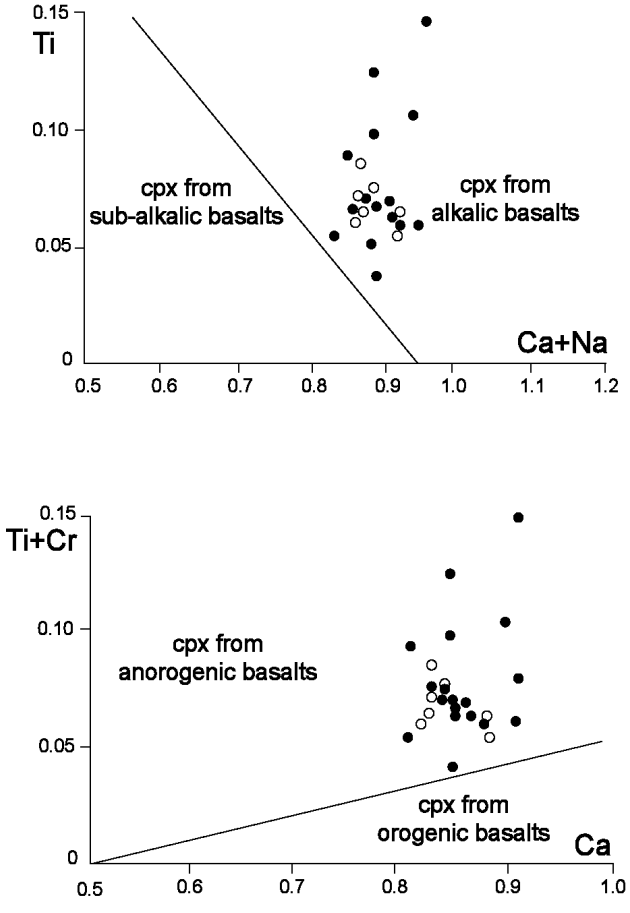

Figure 10. Arperos clinopyroxene analyses plotted on the discrimination diagrams proposed by Leterrier *et al*. (1982).

Using the major immobile elements TiO_2, P_2O_5, and MnO, a tectonomagmatic discrimination diagram for oceanic basalts and basaltic andesites (45 wt%< SiO_2 < 54 wt%; Mullen, 1983) shows that the pillow lavas and the diabasic dikes from the Arperos Formation plot in the field of oceanic island alkaline rocks (Figure 11). Zr and Y are also considered as immobile elements during alteration and metamorphism; a triangular plot of Ti/100-Zr-Yx3 (Pearce and Cann, 1973) shows that these mafic rocks plot in the intra-plate field (Figure 12), and that they are comparable to ocean island alkali basalts. High Ti/V ratios (49-61) of the analyzed samples are also characteristic of alkali basaltic lavas. Shervais (1982) has shown that the fractionation of V from Ti during partial melting and fractional crystallization is a function of oxygen fugacity, and that Ti/V ratios of volcanic rocks increase in the order island-arc volcanic < MORB < alkali basalts. In a Ti-V diagram (Shervais, 1982), the Arperos rocks plot in the field of ocean-island and continental flood basalts (Figure 13).

High Fe_2O_3 values of lavas and dikes (Table 2) are similar to those of tholeiitic lavas, although high-Fe_2O_3 contents have also been reported in alkali basalts from submarine volcanoes (Natland, 1976; Batiza and Vanko, 1984). Mg numbers (Mg # = (Mg/(Mg+Fe) x 100) from the lavas and dikes range between 55 and 62, suggesting a certain degree of fractionation.

The most distinguishing feature of pillow lavas and diabase is their enrichment in rare earth elements (84 ≤ ΣREE ≤ 123 chondritic values) and their slightly enriched light-REE normalized patterns, with $(La/Yb)_N$ ratios ranging from 2 to 4 (REE-normalizing values of Evensen *et al*., 1978), which are in the range of values reported for some alkali and tholeiitic basaltic rocks (2 < $(La/Yb)_N$ < 5, Kay and Gast, 1973). In comparison, island tholeiites from Hawaii and the Galapagos Islands have lower REE abundances (30-50 x chondrites), and lower $(La/Yb)_N$ ratios (2-3) than alkali magmas series.

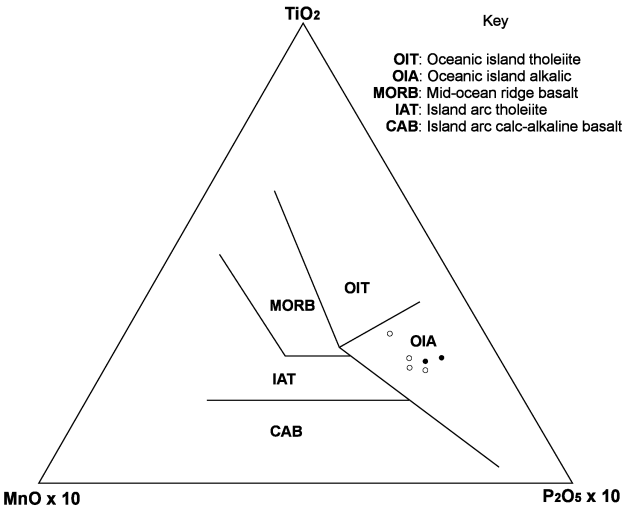

Figure 11. TiO_2-MnO-P_2O_5 tectonomagmatic discrimination diagram (after Mullen, 1983) for the Arperos pillow lavas (full circle) and dikes (circle).

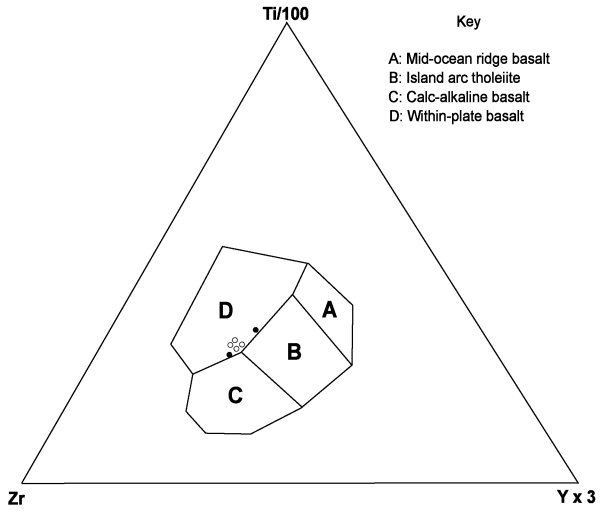

Figure 12. Triangular diagram Ti-Zr-Y (Pearce and Cann, 1973) for-lavas (full circle) and dikes (circle).

Negative Eu anomalies (0.90 < Eu/Eu* < 0.94) in the patterns suggest early fractionation of plagioclase (Figure 14). MORB normalized multielement diagrams show an enrichment in both high field strength (HFS) and large ion lithophile (LIL) elements (Figure 15), which is a typical feature of alkaline intra-plate rocks (Pearce, 1983). La/Yb (1.39-6.30) and Nb/Yb (4.03-5.33) ratios display a narrower range than those reported for enriched-MORBs (E-MORB).

Because their mineralogy (presence of Ti-rich clinopyroxene, substitution types in these ferromagnesian minerals) and the chemical characteristics (high TiO_2, Zr, Nb, P_2O_5, and Ti/V ratios) of the major and trace elements considered as immobile, the Guanajuatito and Barbosa lavas and dikes are considered as mildly alkaline rocks.

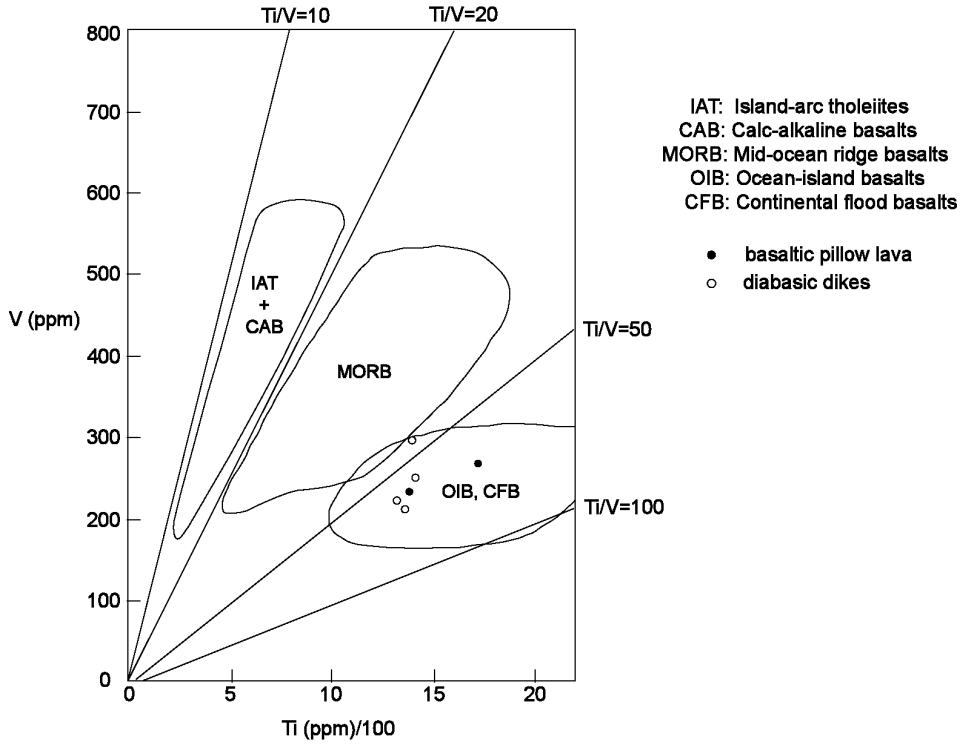

Figure 13. Ti-V diagram (Shervais, 1982) showing the magmatic affinity of the Arperos pillow lavas and diabasic dikes.

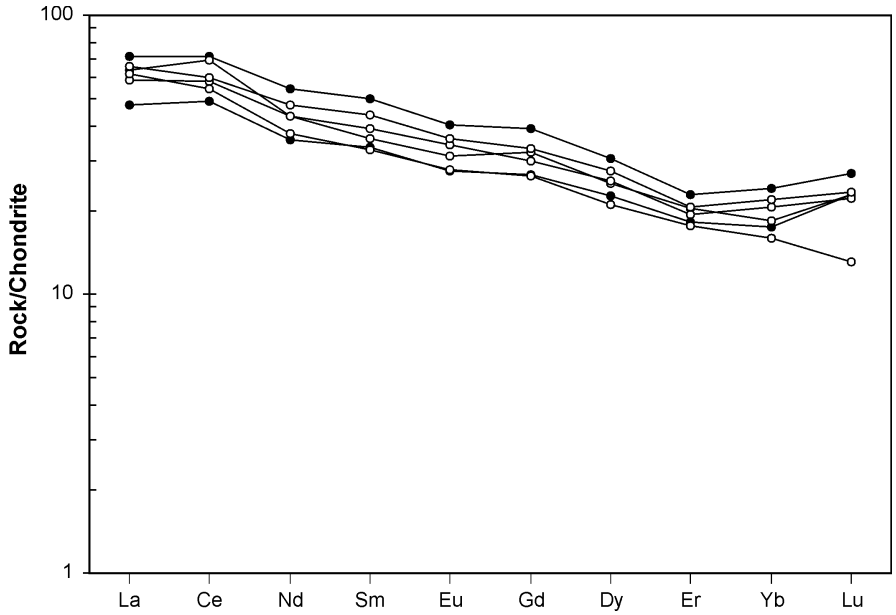

Figure 14. Rare-earth normalized patterns for the Arperos pillow lavas (full circle) and dikes (circle). Normalized REE values after Evensen *et al.* (1978).

CONCLUSIONS AND TECTONIC IMPLICATIONS

There are "pillow lavas and pillow lavas" formed in different tectonic settings. The similar mineralogical and geochemical features of the Arperos basaltic pillow lavas and diabasic dikes suggest that they are mildly alkaline, probably cogenetic rocks, and that they were formed in an anorogenic, oceanic, intra-plate setting. Field relationships show that these rocks are part of a thick (400 m), submarine sequence formed by pillow lavas interbedded with massive lava flows, pillow breccias, hyaloclastites, lapilli tuffs, and diabasic dikes capped by ribbon cherts and other pelagic flysch-like sediments. The Guanajuatito and Barbosa outcrops do not compare well with sections of oceanic crust and ophiolitic sequences, and thus the Arperos Formation should not be considered as a typical ophiolite as proposed by Quintero-Legorreta (1992). Rather, the sequence is considered to be the remnants of intra-plate seamounts. Similar igneous rocks and associated pelagic sediments have been reported for other intra-plate seamounts around the world (Watkins and Browne, 1989; Sliter *et al*., 1991).

Additional evidence supporting that the Arperos sequence was formed over a seamount flank comes from the scarcity of diabasic dikes and sills, the presence of volcaniclastic rocks, and the mixing of carbonate and basaltic material (Staudigel and Schmincke, 1984). Brownish-reddish colors and the presence of carbonates in the pillow horizons suggest that these rocks were formed in a shallow environment, above the CCD. This is also corroborated by the high vesiculation of the pillow lavas, and by the presence of hyaloclastites. On the other hand, abundance of prehnite, and the presence of pumpellyite, albite, and secondary titanite may suggest low grade metamorphism (prehnite-pumpellyite facies) affecting the volcanic and volcaniclastic sequence.

It is generally accepted that within-plate magmatic activity originates from the deep, undepleted, probably metasomatically enriched mantle, which melts in conjuntion with deep mantle plume upwelling. The within-plate volcanism of the Arperos Formation originated from hot-spot activity that affected an oceanic basin (Arperos basin) during Early Cretaceous time. This has important implications for understanding the tectonic setting of volcanosedimentary sequences of central Mexico because the Arperos basin sequence is a major paleogeographic element, extending to the NW (Freydier *et al*., 1996; Freydier *et al.,* 2000) from Guanajuato and to the south of the Transmexican Volcanic Belt. In fact, remnants of similar Early Cretaceous pelagic volcanosedimentary sequences that are sometimes capped by limestones have been reported in the State of Zacatecas (Valdecañas Formation, de Cserna, 1976). Near the town of Pánfilo Natera, pre-Aptian alkalic intra-plate pillow lavas capped by micritic limestones are also present. These sequences are situated along the projected trace of the Mexican thrust belt. These allochthonous fragments of Cretaceous oceanic crust suggest the existence of juxtaposed, accreted terranes in central Mexico, which are now amalgamated by tectonic processes.

The Arperos basin has been considered as formed either in an aseismic ridge near a spreading center (Freydier *et al*., 1996; Freydier *et al*., 2000) or in a back-arc basin

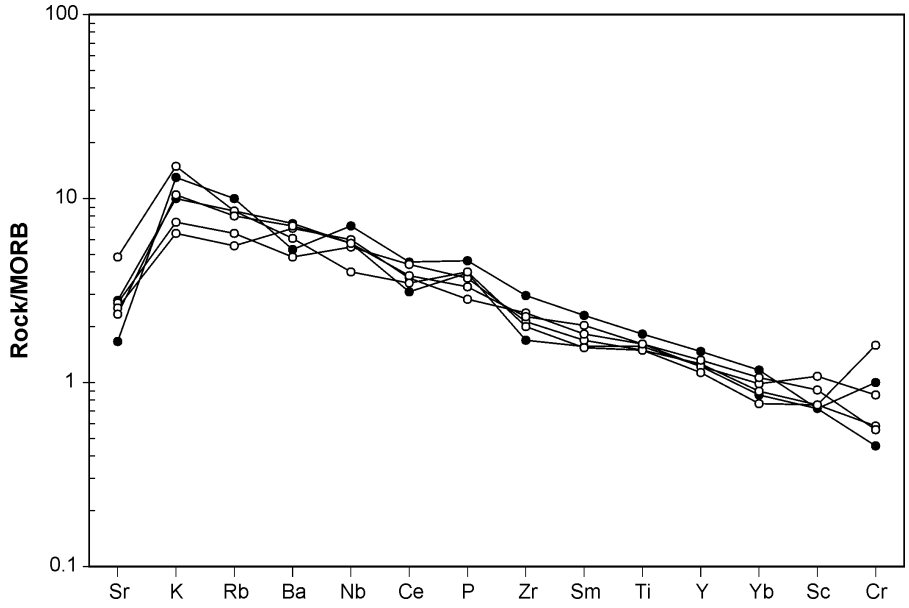

Figure 15. MORB-normalized spidergrams (normalized values of Pearce, 1983) for the lavas (full circle) and dikes (circle).

(Elías-Herrera and Ortega-Gutiérrez, 1998). At present, it is risky to say which one of the two hypotheses is true. Nevertheless, the most important conclusion of this paper is that the Guanajuatito and Barbosa lavas, dikes and associated pelagic sediments are the remnants of intra-plate seamounts, which confirms the intra-oceanic environment of the Mesozoic basament of the Sierra de Guanajuato. This basement is now viewed as an amalgamation of distinct geodynamic environments including: primitive arc-tholeiitic and calc-alkaline intraoceanic magmatic sequences, overlying in tectonic contact mildly alkalic ocean island basalts, which were all formed contemporaneously, during Late Jurassic-Early Cretaceous time. On the other hand, recognition of the seamounts also has important tectonic implications for the evolution of the Guerrero terrane, because these undersea mountains may be part of a seamount chain. We know that the subduction-collision of these topographic highs may be an important mechanism producing accretion, tectonic erosion or volcanic gaps in convergent margins (Ballance *et al.,* 1989).

ACKNOWLEDGMENTS

This research was supported by CONACYT and the Ministère des Affaires Etrangères of France. We are grateful to Henriette Lapierre and Jean Louis Zimmermann for the chemical data and K/Ar radiometric ages, respectively. We would also like to thank Fernando Ortega Gutiérrez of the Instituto de Geología, UNAM and an anonymous reviewer for the correction of the text, and Barbara Martiny for improving the English.

REFERENCES

Ager, D.V., 1993, Mesozoic brachiopods and seamounts, *in* Palfy, J., Vörös, A. (eds.), Mesozoic Brachiopods of Alpine Europe: Budapest, Hungarian Geological Society, p. 1-13.

Almond, D., 1988, Chemical fractionation of titaniferous clinopyroxene from Bayuda, Sudan: Canadian Mineralogist, 26, 1027-1035.

Ballance, P.F., Scholl, D.W., Vallier, T.L., Stevenson, A.J., Ryan, H., Herzer, R.H., 1989, Subduction of a late Cretaceous seamount of the Louisville ridge at the Tonga trench: a model of normal and accelerated tectonic erosion: Tectonics, 8, 953-962.

Barberi, F., Bizcard, H., Varet, J., 1971, Nature of the clinopyroxene and iron-enrichment in alkalic and transitional basalt magmas: Contributions to Mineralogy and Petrology, 33, 93-107.

Basaltic Volcanism Study Project, 1981, Basaltic Volcanism on the Terrestrial Planets (Oceanic Intraplate Volcanism): New York, Pergamon Press, 161-192.

Batiza, R., Vanko, D., 1984, Petrology of young Pacific seamounts: Journal of Geophysical Research, 89, 11235-11260.

Chiodi, M., Monod, O., Busnardo, R., Gaspard, D., Sánchez, A., Yta, M., 1988, Une discordance anté-albienne datée par una faune d´ammonites et de brachiopodes de type téthysien au Mexique central: Geobios, 21, 125-135.

Corona-Chávez, P., 1988, Análisis estratigráfico-estructural de la porción centro-sur de la Sierra de Guanajuato: México, D.F., Instituto Politécnico Nacional, Escuela Superior de Ingeniería y Arquitectura, Tesis profesional, 60 p. (unpublished).

de Cserna, Z., 1976, Geology of the Fresnillo area, Zacatecas, Mexico: Geological Society of America Bulletin, 87, 1191-1199.

Dávila-Alcocer, V.M., Martínez-Reyes, J., 1987, Una edad cretácica para las rocas basales de la sierra de Guanajuato, *in* Simposio sobre la Geología de la Sierra de Guanajuato, Programa y Resúmenes: México, D.F, Universidad Nacional Autónoma de México, Instituto de Geología, 19-20.

Elías-Herrera, M., Ortega-Gutiérrez, F., 1998, The early Cretaceous Arperos oceanic basin (western Mexico). Geochemical evidence for an aseismic ridge formed near a spreading center-Comment: Tectonophysics, 292, 321-326.

Evensen, N.M., Hamilton, P.J., O'Nions, R.K., 1978, Rare-earth abundances in chondritic meteorites: Geochimica and Cosmo-

chimica Acta, 42, 1199-1212.

Freydier, C., Martínez-Reyes, J., Lapierre, H., Tardy, M., Coulon, Ch., 1996, The early Cretaceous Arperos basin (western Mexico): geochemical evidence for an aseismic ridge formed near a spreading center: Tectonophysics, 259, 343-367.

Freydier, C., Martínez-Reyes, J., Lapierre, H., Tardy, M., Coulon, Ch., 1998, The early Cretaceous Arperos Basin (western Mexico): geochemical evidence for an aseismic ridge formed near a spreading center-Reply: Tectonophysics, 292, 327-331.

Freydier, C., Lapierre, H., Ruiz, J., Tardy, M., Martínez-Reyes, J., Coulon, Ch., 2000, The early Cretaceous Arperos basin: an oceanic domain dividing the Guerrero arc from nuclear Mexico evidenced by the geochemistry of the lavas and sediments, *in* Centeno-García, E., Lomnitz, C., Ramírez-Espinoza, J. (eds.), Special Issue, Geologic Evolution of the Guerrero Terrane, Western Mexico: Journal of South American Earth Sciences, 13, 325-336.

Govindaraju, K., Mevell, G., 1987, Fully automated dissolution and separation methods for inductively coupled plasma atomic emission spectrometry rocks analysis. Application to the determination of Rare Earth Elements: Journal of Analytical and Atomic Spectrometry, *2*, 615-621.

Honda, M., McDougall, I., Patterson, D.B., Doulgens, A., Clague, D. A., 1993. Noble gases in submarine pillow basalt glasses from Loihi and Kilauea, Hawaii-a solar component in the Earth: Geochimica et Cosmochimica Acta, 57, 859-874.

Kay, R.W., Gast, P.W., 1973, The rare earth content and origin of alkali-rich basalts: Journal of Geology, 81, 653-682.

Lapierre, H., Ortiz, E., Abouchami, W., Monod, O., Coulon, Ch., Zimmermann, J.L., 1992, A crustal section of an intra-oceanic island arc: the late Jurassic-early Cretaceous Guanajuato magmatic sequence, central Mexico: Earth and Planetary Sciences and Letters, 108, 61-67.

Laughlin, A.W., Poths, J., Healey, H.A., Reneau, S., Wolde, Gabriel, G., 1994, Dating of Quaternary basalts using the cosmogonic ^{3}He and ^{14}C methods with implications for excess ^{40}Ar: Geology, 22, 135-138.

Lemoine, M., Arnaud-Vanneau, A., Arnaud, H., Létolle, R., Mevel, C., Thieuloy, J.P., 1982, Indices possibles de paléo-hydrothermalisme marin dans le Jurassique et le Crétacé des Alpes occidentales (océan téthysien et sa marge continentale européene): essai d´inventaire: Bulletin de la Societé Géologique de France, Série 7, 24, 641-647.

Leterrier, J., Maury, R.C., Thonon, P., Girard, D., Marchal, M, 1982, Clinopyroxene composition as a method of identification of the magmatic affinities of paleo-volcanic series. Earth and Planetary Sciences and Letters, 59, 139-154.

Londsdale, P., Batiza, R., 1980, Hyaloclastite and lava flows on young seamounts examined with a submersible: Geological Society of America Bulletin, 91, 545-554.

Marcelot, G., Bardintzeff, J.M., Maury, R.C., Rançon, J.Ph., 1988, Chemical trends of early-formed clinopyroxene phenocrysts from some alkaline and orogenic basic lavas: Bulletin de la Societé Géologique de France, 4, 851-859.

Monod, O., Lapierre, H., Chiodi, M., Martínez-Reyes, J., Calvet, Ph., Ortiz, E., Zimmermann, J.L., 1990, Réconstitution d'un arc insulaire intra-océanique au Mexique central-la séquence volcano-plutonique de Guanajuato (Crétacé inférieur): Comptes Rendus de l´Académie des Sciences de Paris, Serie II, 310 (1), 45-51.

Mullen, E.D., 1983, $MnO/TiO_2/P_2O_5$: A minor element discriminant for basaltic rocks of oceanic environments and its implications for petrogenesis: Earth and Planetary Sciences and Letters, 62, 53-62.

Natland, J.H., 1976, Petrology of Volcanic Rocks Dredged from Seamounts in the Line Island: Texas, College Station, Texas A&M University, Ocean Drilling Program, Initial Reports of the Deep Sea Drilling Project, 33, 749-777.

Ortiz-Hernández, L.E., Chiodi, M., Lapierre, H., Monod, O., Calvet, Ph., 1992, El arco intraoceánico alóctono (Cretácico Inferior) de Guanajuato-características petrográficas, geoquímicas, estructurales e isotópicas del complejo filoniano y de las lavas basálticas asociadas; implicaciones geodinámicas: Universidad Nacional Autónoma de México, Instituto de Geología, Revista, 9 (2), 126-145.

Ortiz-Hernández, L.E., Martínez-Reyes, J., 1993, Evidence of Cretaceous hot-spot intra-plate magmatism in the central segment of the Guerrero terrane, *in* Ortega-Gutiérrez, F., Coney, P.J, Centeno-García, E., and Gómez-Caballero, A. (eds.), First Circum-Pacific and Circum-Atlantic Terrane Conference, Proceedings: México, Universidad Nacional Autónoma de México, Instituto de Geología, 110-112.

Papike, J.J., Cameron, K.L., Baldwin, K., 1974, Amphiboles and pyroxenes: Characterization of other than quadrilateral components and estimates of ferric iron from microprobe data: Geological Society America, Abstract with Programs, 96, 1053-1054.

Pearce, J.A., Cann, J.R., 1973, Tectonic setting of basic volcanic rocks using Ti, Zr and Y: Earth and Planetary Sciences and Letters, 19, 290-300.

Pearce, J.A., 1983, Role of the sub-continental lithosphere in magma genesis at active continental margins, *in* Hawkesworth, C.J., Norry, M.J. (eds.), Continental Basalts and Mantle Xenoliths: Nantwich, Shiva Publishing, 297-308.

Quintero-Legorreta, O., 1992, Geología de la región de Comanja, estados de Guanajuato y Jalisco: Universidad Nacional Autónoma de México, Instituto de Geología, Revista, 10, 1, 6-25.

Sandy, M.R., 1991, Biostratigraphic affinities of some Jurassic-Cretaceous brachiopod faunas from the Americas and their relation to tectonic and paleoceanographic events, *in* Mckinnon, D.I., Lee, D.E., Campbell, J.D. (eds.), Brachiopod through Time: Rotterdam, A.A. Balkema, 415-422.

Sandy, M.R., Blodgett, R.B., 1996, *Peregrinella* (Brachiopoda; Rhynchonellida) from the Early Cretaceous, Wrangellia terrane, Alaska, *in* Copper, P., Jin, J. (eds.), Brachiopods; Proceedings of the 3rd International Brachiopod Congress Sudbury, Ontario, Canada: Rotterdam, A.A. Balkema, 239-242.

Shervais, J.W., 1982, Ti/V plots and the petrogenesis of modern and ophiolitic lavas: Earth and Planetary Sciences and Letters, 59, 53-71.

Sliter, W.V., Murchey, B.L., McLaughlin, R.J., Kistler, R.W., 1991, Permanent terrane: history of Early Cretaceous seamount formation: Geological Society of America, Abstracts with Programs, 23, 98.

Staudigel, H., Schmincke, H.S., 1984, The Pliocene seamount of La Palma/Canary Islands: Journal of Geophysical Research, 89, 11195-11215.

Tracy, R.I., Robinson, P., 1977, Zoned titanian augite in alkali olivine basalts from Tahiti and the nature of titanium substitutions in augite: American Mineralogist, 62, 634-645.

Wass, S.Y., 1979, Multiple origins of clinopyroxenes in alkali basaltic rocks: Lithos, 12, 115-132.

Watkins, R., Browne, Q.J., 1989, An Ordovician continental-margin sequence of turbidite and seamount deposits in the Roberts Mountains allochthon, Independence Range, Nevada: Geological Society of America Bulletin, 101, 731-741.

Manuscript received: January 10, 2001
Corrected manuscript received: June 6, 2002
Manuscript accepted: July 2, 2002